ACS OMEGA

Article

Cite This: ACS Omega 2018, 3, 13275−13282

http://pubs.acs.org/journal/acsodf

Resveratrol Sustains Insulin-Degrading Enzyme Activity toward Aβ42

Claire A. Krasinski, Valerie A. Ivancic, Qiuchen Zheng, Donald E. Spratt, and Noel D. Lazo*

Carlson School of Chemistry and Biochemistry, Clark University, 950 Main Street, Worcester, Massachusetts 01610, United States

Supporting Information

ABSTRACT: Alzheimer's disease (AD), the most common cause of dementia in the elderly, is the sixth leading cause of death in the United States. We hypothesize that the impaired clearance of Aβ42 from the brain is partly responsible for the onset of sporadic AD. In this work, we evaluated the activity of insulin-degrading enzyme (IDE) toward Aβ42 in the presence of resveratrol, a polyphenol found in red wine and grape juice. By liquid chromatography/mass spectrometry, we identified initial cleavage sites in the absence and presence of resveratrol that carry biological relevance connected to the amyloidogenic properties of Aβ42. Incubation with resveratrol results in a substantial increase in Aβ42 fragmentation compared to the control, signifying that the polyphenol sustains IDE-dependent degradation of Aβ42 and its fragments. Our findings suggest that therapeutic and/or preventative approaches combining resveratrol and IDE may hold promise for sporadic AD.

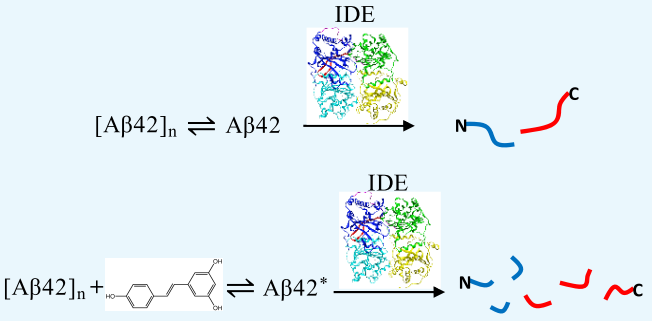

INTRODUCTION

Alzheimer's disease (AD) is the leading cause of dementia in the aged. According to the Alzheimer's Association, AD currently affects 5.7 million Americans.[1] This statistic is projected to increase to 14 million by 2050.[1] One popular target of basic science research and clinical trials is amyloid-β(1−42) (Aβ42), which is hypothesized to play an initiating role in AD.[2] Under certain conditions, Aβ42 aggregates to form neurotoxic oligomers.[3] Researchers have long hypothesized that the increased production of pathogenic Aβ42 causes AD, though this appears to account for only 10% of AD cases.[2] About 90% of AD patients have the sporadic form, which may instead arise from impaired degradation or clearance of Aβ42 from the brain.[2]

In this work, we propose the combination of two key components implicated in improving the efficiency of this process and preventing Aβ42 accumulation. One component of interest is insulin-degrading enzyme (IDE, EC No. 3.4.24.56), a 110 kDa, Zn^{2+} metalloprotease that plays a significant role in the extracellular and intracellular degradation of Aβ.[4,5] The unique structure of IDE can accommodate a wide variety of monomeric substrates of similar size (<80 amino acids), including Aβ, insulin, glucagon, and amylin.[6] IDE consists of four domains (labeled 1−4 in Figure 1). The N-terminal half (IDE^N, composed of domains 1 and 2) is attached by a flexible linker to the C-terminal half (IDE^C, composed of domains 3 and 4). Biochemical,[7−10] crystallographic,[6,11] and cryogenic electron microscopic[12] studies have provided the basis for substrate recognition by IDE. During its catalytic cycle, IDE exists in two conformations: open IDE allows the entry of substrates into IDE's catalytic chamber and

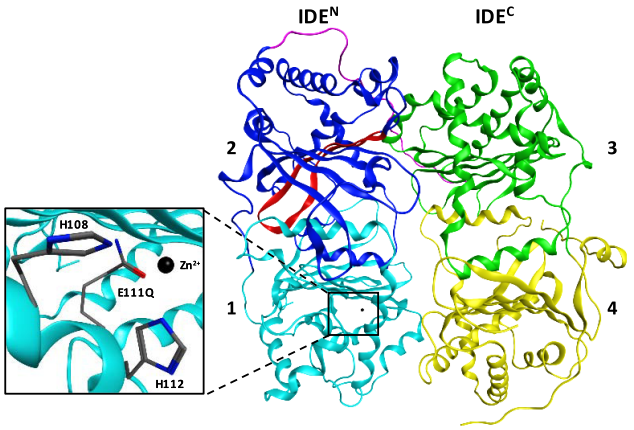

Figure 1. Insulin-degrading enzyme (4PES)[11] is composed of four domains. The N-terminal half of IDE (IDE^N, domains 1 and 2) is linked to the C-terminal half (IDE^C, domains 3 and 4) by a flexible linker (purple). Domain 1 contains Zn^{2+} coordinated to H108 and H112 and the catalytically active residue (E111, mutated to a glutamine in 4PES). Domain 2 contains a highly conserved exosite (red) that is hypothesized to be important for the binding of substrates prior to degradation.

the release of products, whereas close IDE performs the hydrolysis of peptide bonds. The negatively charged IDE^N has a highly conserved exosite about 30 Å away from Zn^{2+} coordinated to H108 and H112, and a catalytically active

Received: August 6, 2018
Accepted: October 2, 2018
Published: October 16, 2018

DOI: 10.1021/acsomega.8b01913
ACS Omega 2018, 3, 13275−13282

E111 (Figure 1), whereas the positively charged IDE^C is hypothesized to permit initial contact with substrates. One proposed mechanism by Guo and co-workers states that IDE-dependent degradation occurs via E111-catalyzed hydrolysis after the substrate anchors to IDE's exosite by its N-terminus and unfolds.[7] Although several enzymes cleave Aβ,[13] evidence suggests that IDE plays a key role in the maintenance of Aβ homeostasis.[5] Aβ accumulation has been observed in both IDE-knockout mice[14,15] and individuals with early stages of sporadic AD.[16] This implies that a decline in IDE expression and/or activity with age may be a contributing factor for increased aggregation of Aβ42 and formation of neurotoxic oligomers. Therefore, the development of therapeutic strategies focusing on IDE is warranted.

To this end, we are curious about the therapeutic potential of simultaneously using IDE and polyphenols, a second component of interest, to target Aβ42. Polyphenols are naturally occurring compounds, many of which can cross the blood−brain barrier.[17] Mounting in vitro and in vivo evidence shows that polyphenols are neuroprotective in that they diminish brain neuropathology and ameliorate cognitive function in animal models of AD through several mechanisms.[17,18] In this work, we chose resveratrol (3,5,4′-trihydroxystilbene), a polyphenol found in red wine and grape juice.[19] Resveratrol exists in the cis- and trans-configurations (Figure 2), but the latter is more stable and is

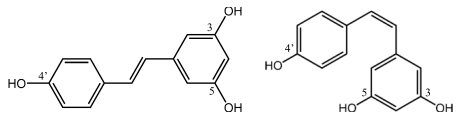

Figure 2. Resveratrol has two isomers. *trans*-Resveratrol (left) is more stable and potent than *cis*-resveratrol (right).

known to be responsible for the beneficial effects of the compound.[20] Moderate consumption of red wine has been associated with a lower risk of dementia.[21] More recently, Krikorian et al. found that dietary supplementation with grape juice significantly improves the memory of subjects with mild cognitive impairment.[22,23] Moderate consumption of red wine reduces amyloid plaque pathology in a transgenic mice model of AD.[24] Vingtdeux et al. demonstrated that orally administered resveratrol in mice reduces Aβ levels and deposition in the cerebral cortex.[25] Porquet et al. reported that dietary resveratrol reduces amyloid burden, tau hyperphosphorylation, and cognitive impairment in SAMP8 mice, a model of age-related AD.[26] According to Ladiwala et al., resveratrol acts by remodeling three conformers of Aβ42, including soluble oligomers, fibrillar intermediates, and fibrils, into unstructured, nontoxic aggregated species.[27] Fu and co-workers probed the ability of resveratrol to interact with Aβ42 oligomers using atomic force microscopy and NMR spectroscopy, and observed that resveratrol binds to the N-terminus of Aβ monomers and limits oligomer formation to low-molecular-weight oligomers.[28]

Despite these findings supporting resveratrol's ability to modulate Aβ aggregation and deposition, the direct effect of the polyphenol on IDE-dependent degradation of Aβ is not known. Marambaud et al. reported that although resveratrol promotes clearance of Aβ40 and Aβ42 by the proteasome, Aβ levels were not rescued when resveratrol-treated HEK293 cells were pretreated with insulin, believed to be a competitive IDE inhibitor by the authors.[29] This result led them to conclude that resveratrol does not facilitate Aβ degradation by IDE, among other enzymes.[29] In contrast, Rege et al. demonstrated that a 2 h resveratrol pretreatment rescues Aβ40-induced decline in IDE expression exhibited by rat hippocampal neuronal cells, suggesting that resveratrol may aid degradation through an indirect manner via increased IDE expression.[30] In this work, we used two in vitro systems, one comprised of Aβ42 and IDE (control) and the other comprised of Aβ42, resveratrol, and IDE, to directly examine the effect of resveratrol on IDE-dependent degradation of Aβ42. Our results show that IDE is active toward Aβ42 in the presence of resveratrol, and that resveratrol sustains the activity of IDE toward the primary fragments of Aβ42.

RESULTS AND DISCUSSION

We first pretreated Aβ42 and expressed and purified IDE using procedures adapted from Fradinger et al.[31] and Farris et al.,[32] respectively. Thereafter, IDE-dependent digestions of Aβ42 with and without resveratrol were conducted using a substrate-to-enzyme molar ratio of 100:1 and a digestion temperature of 4 °C. We used a temperature of 4 °C for two important reasons: (1) to delay the onset of fibril formation[33] and (2) to control the proteolysis[34] so that we can unambiguously identify the primary fragments resulting from initial cleavages in Aβ42. To characterize the digests, we first used circular dichroism (CD). Aliquots of each digestion were then removed at specific time points, and the reactions were quenched by acidification to low pH (<2.0) and stored at −20 °C until analysis by liquid chromatography/mass spectrometry (LC/MS).

CD spectra of Aβ42 in 10 mM phosphate buffer (pH 7.4) in the absence (Figure S1A) and presence of resveratrol (Figure S1B) at 4 °C show minima below 200 nm, consistent with the dominant presence of unstructured Aβ42 in the samples. This result together with the micromolar concentration of Aβ42 (i.e., 25 μM) indicate that our preparations contain a mixture of monomers and oligomers, as described by Lazo et al.[35] We did not observe significant changes in the spectra shown in Figure S1A and B over 6 days of incubation, indicating that Aβ42 remained predominantly unstructured. CD spectra of digests at 4 °C in the absence (Figure S2A) and presence (Figure S2B) of resveratrol recorded periodically over the digestion period suggest the presence of random coil peptides.

To evaluate the activity of IDE toward Aβ42 at pH 7.4 and 4 °C, we first identified the initial cleavage sites in the substrate in the absence and presence of resveratrol. Figure 3A,B presents the mass spectra of fragments of Aβ42 resulting from initial cleavages in the absence of resveratrol. Fragments D1−F19 and D1−F20 were detected (Figure 3A and Table 1), along with F20−A42 and A21−A42 (Figure 3B and Table 1). These results indicate initial cleavages at the peptide bonds between Phe19 and Phe20 and Phe20 and Ala21 (Figure 3C). Since IDE only degrades monomeric substrates,[6] our results provide unambiguous evidence for Aβ42 monomers in dynamic equilibrium with Aβ42 oligomers, which are then degraded by IDE

$$\text{A}\beta\text{42 oligomers} \rightleftharpoons \text{A}\beta\text{42 monomers} \xrightarrow{\text{IDE}} \text{A}\beta\text{42 fragments}$$

Comparison of the peptide maps shown in Figure 3C with those obtained by others is difficult to make, primarily because they employed digestion conditions that do not match ours.

DOI: 10.1021/acsomega.8b01913
ACS Omega 2018, 3, 13275−13282

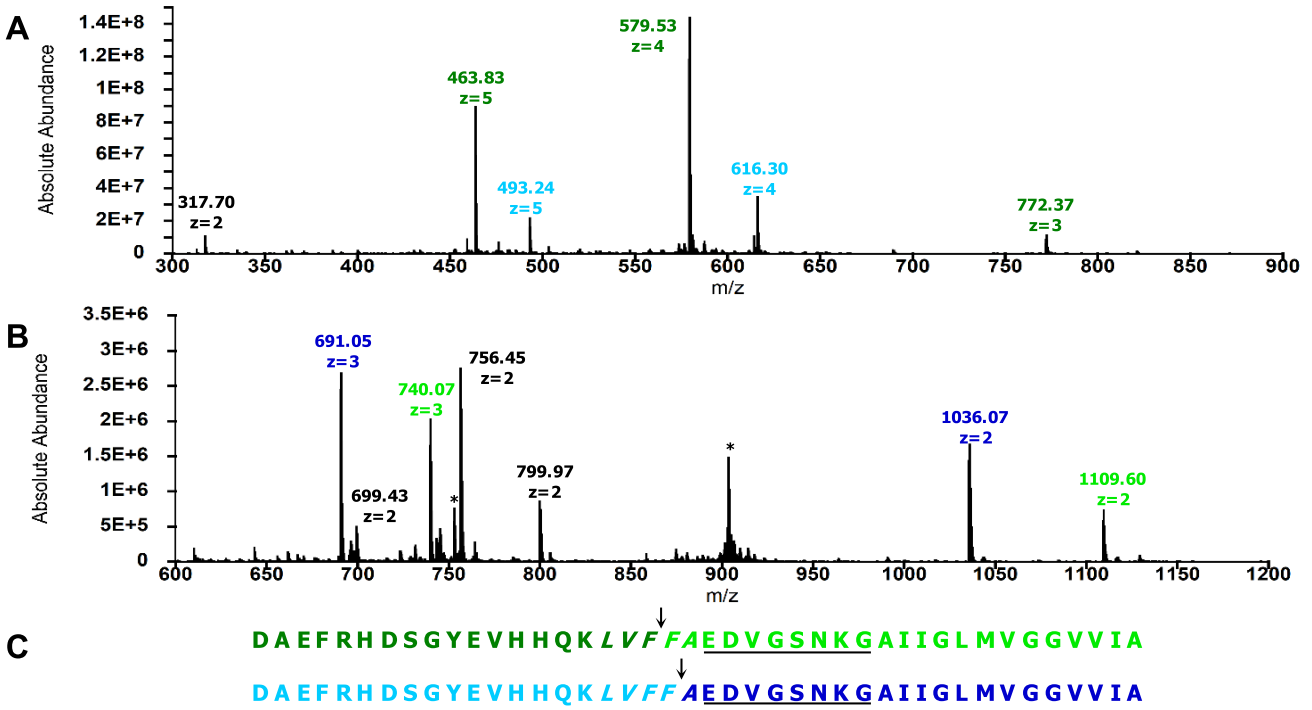

Figure 3. Initial cleavage sites in Aβ42 resulting from IDE-dependent degradation in the absence of resveratrol. (A) Mass spectrum of the primary N-terminal fragments (colored accordingly), which have retention times of 26−31 min. The peak at 317.70 corresponds to A30−M35ox. (B) Mass spectrum of the primary C-terminal fragments (colored accordingly), which have retention times of 40−43 min. Peaks labeled with asterisks correspond to Aβ42. (C) Peptide maps of Aβ42 depicting initial cleavages at the peptide bonds between Phe19 and Phe20 and between Phe20 and Ala21, corresponding to the color-coded fragments in (A) and (B). Residues in the central hydrophobic cluster (CHC) and loop region are italicized and underlined, respectively.

Table 1. Fragments of Aβ42 Resulting from Initial Cleavages by IDE at pH 7.4, 4 °C and Substrate-to-Enzyme Molar Ratio of 100:1

fragments	observed m/z ratio	charge z	observed mass (Da)	theoretical mass (Da)	δ (Da)[a]	initial cleavage site
D1−F19	463.83	5	2314.15	2314.50	−0.35	Phe19−Phe20
	579.53	4	2314.12		−0.38	
	772.37	3	2314.11		−0.39	
F20−A42	740.07	3	2217.21	2217.61	−0.40	
	1109.60	2	2217.20		−0.41	
D1−F20	493.24	5	2461.20	2461.68	−0.48	Phe20−Ala21
	616.30	4	2461.20		−0.48	
A21−A42	691.05	3	2070.15	2070.43	−0.28	
	1036.07	2	2070.14		−0.29	
D1−K28[b]	653.31	5	3261.55	3262.50	−0.95	Lys28−Gly29
G29−A42[b] oxidized[c]	643.38	2	1284.76	1285.75	−1.01	

[a]Observed mass−theoretical mass. [b]Primary fragments observed only in the presence of resveratrol. [c]Met35 oxidized to a sulfoxide.

For example, Rogeberg et al. used rat IDE, a digestion temperature of 37 °C and a higher amount of IDE (substrate-to-enzyme ratio of 25:1).[36] Mukherjee et al. also used rat IDE to digest Aβ40 and Aβ42 at 37 °C at unspecified substrate-to-enzyme ratios.[37] Guo et al. investigated the digestion of Aβ40 by human IDE at 37 °C and a substrate-to-enzyme ratio of 50:1.[7] Song et al. also studied the degradation of Aβ40 by rat IDE at 37 °C at unspecified substrate-to-enzyme ratios.[38] Hubin et al. found that at 37 °C, Aβ can be cleaved by IDE at least twice, complicating the identification of the initial cleavage sites.[39] Nonetheless, we noted that the peptide maps of Aβ42 and Aβ40 presented in these studies are similar to Figure 3C in that they also show the peptide bonds between Phe19 and Phe20 and between Phe20 and Ala21 as initial cleavage sites.

In the presence of resveratrol, fragments D1−F19, D1−F20, and D1−K28 were detected (Figure 4A and Table 1) together with fragments F20−A42, A21−A42, and G29−A42ox (Figure 4B and Table 1). These data indicate that in addition to initial cleavages at the peptide bonds between Phe19 and Phe20 and Phe20 and Ala21, the peptide bond between Lys28 and Gly29 is also cleaved initially in the presence of resveratrol (Figure 4C). Together, these results signify that IDE is active in the presence of resveratrol.

The two initial cleavages at the peptide bonds between Phe19 and Phe20 and Phe20 and Ala21 (Figures 3C and 4C) occur in $L_{17}VFFA_{21}$, known as the central hydrophobic cluster

DOI: 10.1021/acsomega.8b01913
ACS Omega 2018, 3, 13275−13282

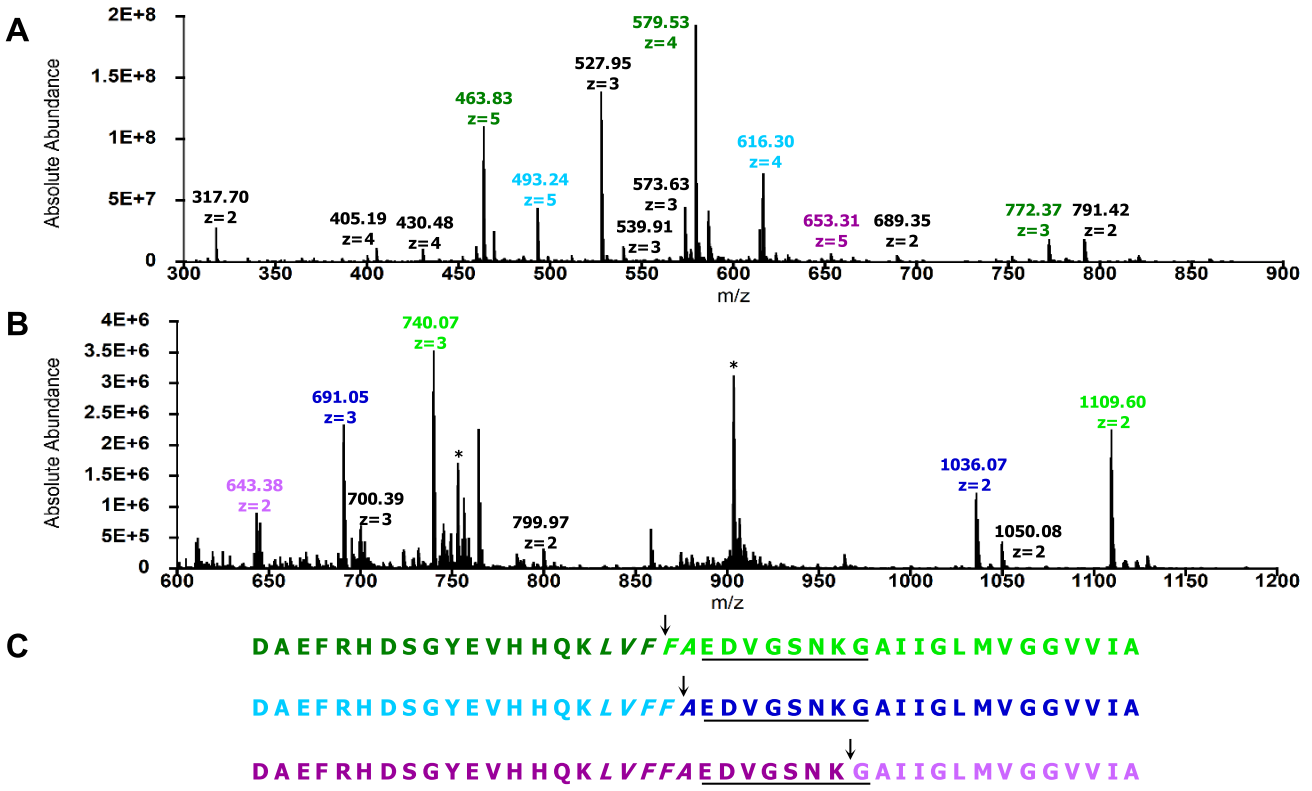

Figure 4. Initial cleavage sites in Aβ42 resulting from IDE-dependent degradation in the presence of resveratrol. (A) Mass spectrum of the primary N-terminal fragments (colored accordingly), which have retention times of 25−30 min. Peaks labeled in black correspond to secondary fragments. (B) Mass spectrum of the primary C-terminal fragments (colored accordingly), which have retention times of 40−43 min. Peaks labeled with asterisks correspond to Aβ42. (C) Peptide maps of Aβ42 depicting initial cleavages at the peptide bonds between Phe19 and Phe20, between Phe20 and Ala21, and between Lys28 and Gly29, corresponding to the color-coded fragments in (A) and (B). Residues in the CHC and loop region are italicized and underlined, respectively.

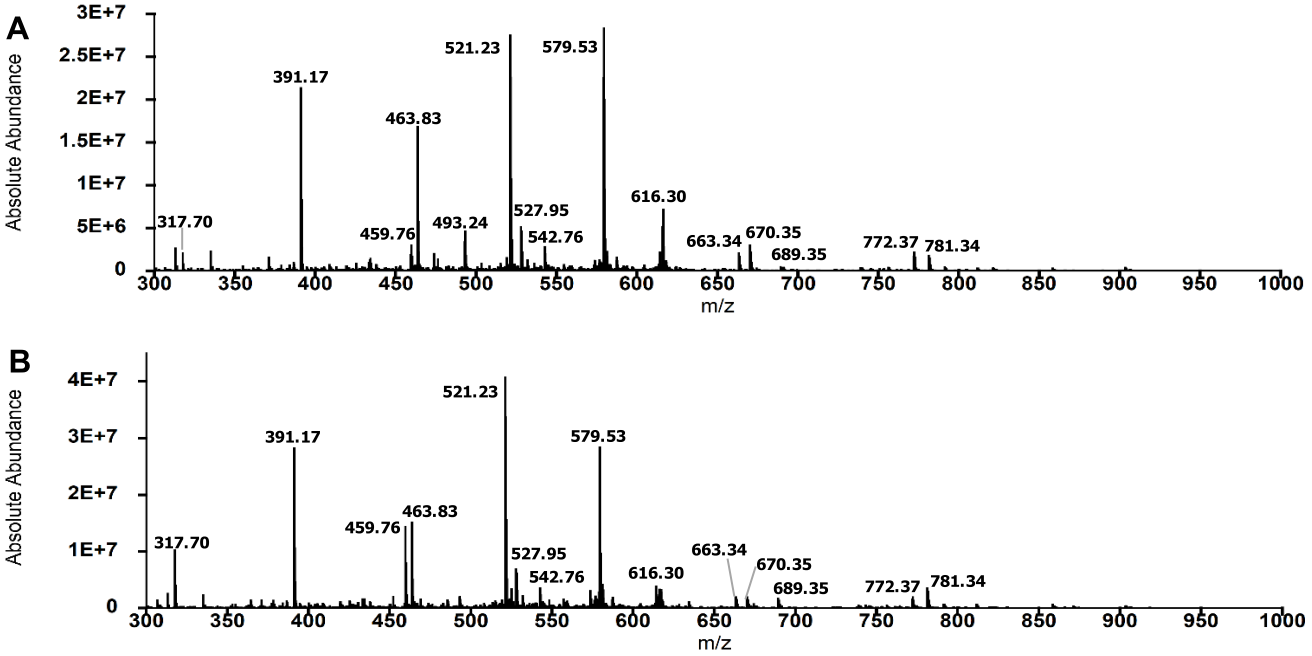

Figure 5. Primary fragments of Aβ42 were not degraded significantly by IDE at pH 7.4 and 4 °C. (A) Total mass spectrum of the 2 h digest shows the dominant presence of peaks corresponding to Aβ42 fragments resulting from initial cleavages. (B) Total mass spectrum of the 6 h digest is essentially similar to the spectrum of the 2 h digest. Dominant peaks in (A) and (B) are labeled by their m/z ratios (also detailed in Tables S1 and S2).

DOI: 10.1021/acsomega.8b01913
ACS Omega 2018, 3, 13275−13282

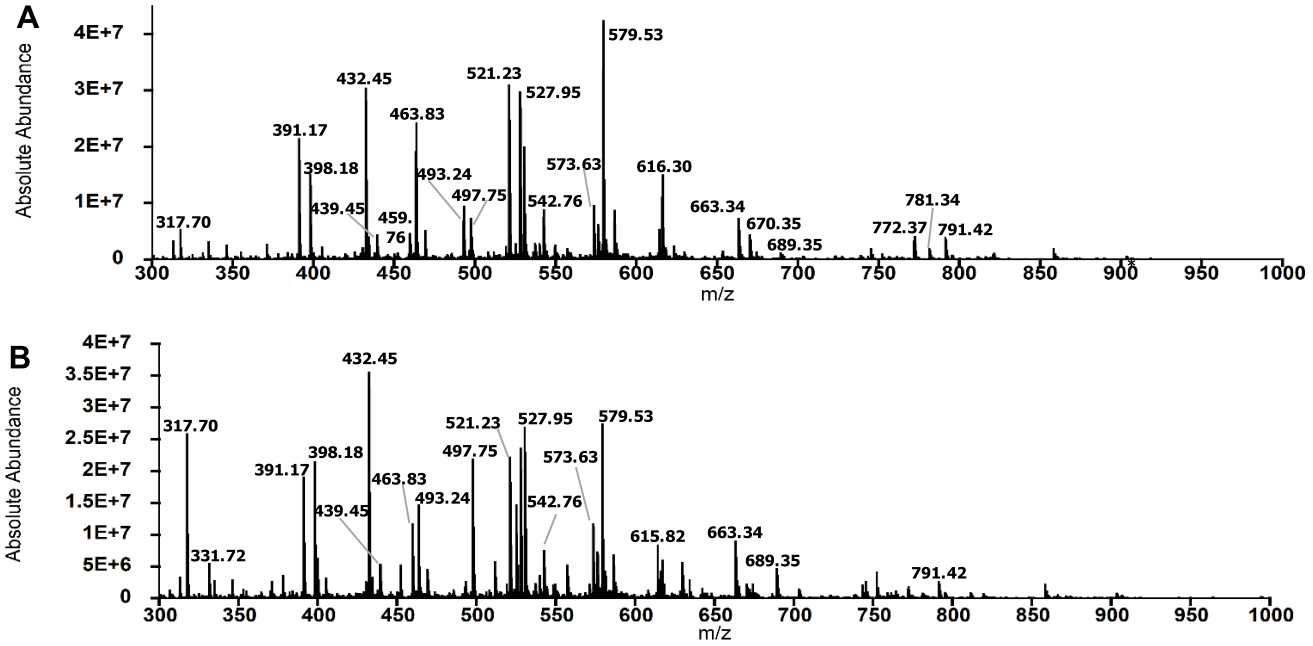

Figure 6. Primary fragments of Aβ42 were degraded significantly by IDE in the presence of resveratrol at pH 7.4 and 4 °C. (A) Total mass spectrum of the 2 h digest shows the presence of peaks due to primary Aβ42 fragments resulting from initial cleavages and peaks corresponding to secondary fragments resulting from further degradation of the primary fragments. (B) Total mass spectrum of the 6 h digest shows significant changes relative to the spectrum in (A), including alterations in peak intensities and the appearance of new peaks. Dominant peaks in (A) and (B) are identified by their m/z ratios (also detailed in Tables S3 and S4).

(CHC) of Aβ42. This result correlates well to the detection of truncated Aβ peptides, including Aβ(1−19) and Aβ(1−20) in cerebrospinal fluid[40] and in plasma from AD patients and controls.[41] The mechanism of IDE-dependent degradation of Aβ42 is not completely understood, but the current working model speculating that the N-termini of substrates interact with the negatively charged glutamate residues at or near IDE's exosite[7] appears to be consistent with cleavages occurring in the CHC. Importantly, by cleaving in the CHC, IDE prevents the intramolecular association of the cluster with the hydrophobic segment $A_{30}IIGL_{34}$ of Aβ42, a key interaction in the three-dimensional structure of a disease-relevant Aβ42 fibril.[42]

The additional initial cleavage site in the presence of resveratrol, i.e., at the peptide bond between Lys28 and Gly29, occurs in the putative loop region of Aβ42, i.e., $E_{22}DVGSNKG_{29}$, which facilitates the interaction of the CHC with $A_{30}IIGL_{34}$.[42] Using a panel of enzymes that includes chymotrypsin (EC No. 3.4.21.1), endoproteinase Asp-N (EC No. 3.4.24.33), endoproteinase Glu-C (EC No. 3.4.21.19), human neutrophil elastase (EC No. 3.4.21.37), porcine pancreatic elastase (EC No. 3.4.21.36), thermolysin (EC No. 3.4.24.27), and trypsin (EC No. 3.4.21.4), Lazo et al. showed that $E_{22}DVGSNKG_{29}$ is protease-resistant.[35] By cleaving a peptide bond in the loop region of Aβ42, IDE prevents the association of the CHC and $A_{30}IIGL_{34}$ segment implicated in the formation of the repeating Aβ42 fold in pathologic Aβ42 fibrils.[42]

Next, we determined if resveratrol sustains the activity of IDE toward the primary fragments of Aβ42. Figure 5 presents the total mass spectra of the 2 and 6 h digests in the absence of resveratrol. We noted that the two spectra are similar in terms of the number of peaks and intensities of the major peaks, indicating that further degradation of the primary N- and C-terminal fragments of Aβ42 did not occur significantly over the 4 h time interval. We identified 19 and 22 secondary fragments in the 2 and 6 h digests, respectively (Tables S1 and S2). Figure 6 shows the total mass spectra of the 2 and 6 h digests in the presence of resveratrol. In contrast to Figure 5, the spectra are more complex in that there are more peaks corresponding to fragments produced by cleavages in the primary fragments. We identified 31 secondary fragments at 2 h and 33 secondary fragments at 6 h (Figure 6, Tables S3 and S4). Prominent peaks in the spectra in Figure 6 that were not detected or of low intensities in the control spectra (Figure 5) included peaks at 398.18 (H14−N27), 432.45 (F20−V36), 497.75 (L17−G25), and 527.95 (Q15−K28) (Tables S3 and S4). We also observed significant changes in the intensities of peaks in the mass spectra of the 2 and 6 h digests in the presence of resveratrol. For example, the intensity of the peak at 317.70, corresponding to A30−M35ox, increased, whereas the intensity of the peak at 616.30, corresponding to D1−F20, decreased. Together, these results show that resveratrol sustains the activity of IDE toward the primary fragments of Aβ42.

In summary, our work clearly shows that unstructured Aβ42 monomers undergo proteolysis by IDE in the presence and absence of resveratrol. The initial cleavage sites across samples are similar and hold biological relevance in that they preclude the folding of Aβ42 into a conformer implicated in the formation of pathologic Aβ42 fibrils. However, the presence of resveratrol also renders the putative loop region of Aβ42 susceptible to initial cleavage. Additionally, our work shows that when resveratrol is present, the fragmentation of the primary fragments of Aβ42 is significantly increased. These unambiguous outcomes with resveratrol may arise from two mechanisms. First, several studies have shown that the catalytic activity of IDE is allosterically regulated. Such regulation can be driven by ATP,[43,44] its substrate,[12] allosteric mutations in the enzyme,[10] anions,[45] small peptides, including dynorphin[46]

DOI: 10.1021/acsomega.8b01913
ACS Omega 2018, 3, 13275−13282

and somatostatin,[47] and small molecules.[48,49] Second, although resveratrol does not prevent oligomer formation, it can selectively remodel soluble toxic Aβ42 oligomers into off-pathway conformers[27] that may drive the dynamic equilibrium discussed above to IDE-degradable monomers. Both mechanisms likely contribute, but we speculate that one dominates depending on whether the substrate is Aβ42 monomer or its primary fragments. The detailed mechanism of the sustainment of the activity of IDE by resveratrol awaits future structural studies of IDE in the presence of resveratrol, Aβ42, and its primary fragments. Such studies may be accomplished using cryoEM, which was recently applied to IDE in the presence of insulin.[12]

In conclusion, in addition to increasing hippocampal IDE expression in vivo,[30] resveratrol also sustains the activity of IDE toward Aβ42 monomer and its fragments. Interestingly, we have produced kinetic data showing that resveratrol does not affect the IDE-dependent degradation of insulin (Lazo et al., unpublished results). These results imply that resveratrol may be specific to Aβ and will not have off-target effects. If true, the combination of resveratrol and IDE may address the impaired Aβ42 clearance in the brain, which is thought to be primarily responsible for sporadic cases of AD.

EXPERIMENTAL SECTION

Pretreatment of Aβ42. Aβ42 (≥95% pure by HPLC, 21st Century Biochemicals, Marlborough MA) was pretreated as 1 mg/mL solutions with 100% 1,1,1,3,3,3-hexafluoro-2-isopropanol and then 2 mM NaOH using a protocol by Fradinger et al.[31] Pretreated Aβ42 was stored at −20 °C until experimentation.

Expression and Purification of Human Insulin-Degrading Enzyme. Glutathione S-transferase-tagged human insulin-degrading enzyme (GST-IDE in pGEX-6p-1 vector, from Dr Malcolm A. Leissring) was overexpressed and purified using procedures adapted from Farris et al.[32] Briefly, we transformed GST-IDE into *Escherichia coli* BL21-CodonPlus (DE3) competent cells. Expression was initiated with 50 μM IPTG, and the cells were grown overnight at 25 °C. Prior to lysing the cells, phenylmethylsulfonyl fluoride nonmetalloprotease inhibitor was added. A 5 mL GST Trap Fast Flow column (GE) on an ÄKTA Pure fast protein liquid chromatography (FPLC, GE) was used to purify GST-IDE, which was eluted with phosphate-buffered saline (PBS) and 10 mM glutathione. A HiLoad 16/600 Superdex S-200 pg gel filtration column connected to an ÄKTA Pure FPLC further purified IDE. The molar extinction coefficient of IDE at 280 nm,[50] $\varepsilon_{280\ nm}$ = 113570 M^{-1} cm^{-1}, was used to determine purified protein concentration. IDE aliquots with 1% glycerol (v/v) were flash-frozen and stored at −80 °C in PBS (pH 7.4). We confirmed IDE activity by CD/LC/MS using insulin as a positive control substrate.

Preparation of Stock Solutions. Pretreated Aβ42 (~0.25 mg) was rehydrated in 10 mM phosphate buffer (pH 7.4) to a concentration of 1 mg/mL. On ice, the pH of the Aβ42 stock solution was adjusted to 7.4 with the addition of 1 M HCl. A stock solution (0.5 mg/mL) of *trans*-resveratrol (>99% pure by GC, Sigma-Aldrich, St. Louis MO) was prepared in 100% ethanol. The concentrations of the stock solutions of Aβ42, resveratrol, and IDE were determined by UV−vis spectroscopy, using the molar extinction coefficients of $\varepsilon_{275\ nm}$ = 1390 M^{-1} cm^{-1},[35] $\varepsilon_{306\ nm}$ = 26800 M^{-1} cm^{-1},[51] and $\varepsilon_{280\ nm}$ = 113570 M^{-1} cm^{-1},[50] respectively.

Circular Dichroism (CD) Spectroscopy. Six samples, each with a volume of 350 μL, were prepared for CD analysis: (1) Aβ42 only (25 μM), (2) IDE only (0.25 μM), (3) Aβ42 plus IDE (25 μM Aβ42 + 0.25 μM IDE or 100:1 substrate-to-enzyme molar ratio), (4) Aβ42 and resveratrol (25 μM Aβ42 + 40 μM resveratrol), (5) IDE and resveratrol (0.25 μM IDE + 40 μM resveratrol), and (6) Aβ42, resveratrol and IDE (25 μM Aβ42 + 40 μM resveratrol + 0.25 μM IDE). CD samples were incubated in quartz cuvettes (path length 1 mm) at 4 °C. Measurements were recorded on a Jasco J-815 spectrometer from 260 to 198 nm at 4 °C with 1 nm steps and averaged over eight accumulations. The Savitzsky−Golay method (convolution width = 9) was used to smoothen all spectra.

Liquid Chromatography/Mass Spectrometry (LC/MS). Aliquots (18 μL) of CD samples #3 (Aβ42 plus IDE) and #6 (Aβ42, resveratrol and IDE) were removed periodically, and the reactions were quenched with 8 μL of 1% trifluoroacetic acid in H_2O. Quenched 2 and 6 h digestions were subjected to LC/MS at the University of the Massachusetts Medical School's Proteomics and Mass Spectrometry Facility. Chromatography was accomplished using a NanoAcquity (Waters, Milford MA) UPLC system equipped with a Michrom Magic C18AQ column. Mass spectrometry was performed using an Orbitrap Q Exactive hybrid mass spectrometer (Thermo Fisher, Waltham MA). Spectra were acquired from m/z 300 to 1750 at 70 000 resolution, and data-dependent acquisition chose the top 10 most abundant precursor ions for tandem mass spectrometry by higher-energy collisional dissociation fragmentation.

ASSOCIATED CONTENT

Supporting Information

The Supporting Information is available free of charge on the ACS Publications website at DOI: 10.1021/acsomega.8b01913.

CD spectra of Aβ42 in the presence and absence of resveratrol; CD spectra of Aβ42 digests in the absence and presence of resveratrol; tables of secondary fragments produced by IDE-dependent degradation of Aβ42 (PDF)

AUTHOR INFORMATION

Corresponding Author

*E-mail: nlazo@clarku.edu.

ORCID

Noel D. Lazo: 0000-0003-1769-7572

Author Contributions

C.A.K. and Q.Z. performed all digestion experiments; C.A.K. and V.A.I. produced and purified IDE under the guidance of D.E.S.; C.A.K. analyzed MS data; C.A.K. wrote the first draft of the manuscript, and all authors participated in the editing process; N.D.L. supervised the project and writing of the manuscript.

Funding

This work was funded by the National Institutes of Health (R15AG055043 to NDL).

Notes

The authors declare no competing financial interest.

DOI: 10.1021/acsomega.8b01913
ACS Omega 2018, 3, 13275−13282

■ ACKNOWLEDGMENTS

Dr Malcolm A. Leissring of UC Irvine is acknowledged for kindly providing the bacterial expression vector and protocol for the production of IDE.

■ REFERENCES

(1) Alzheimer's Disease Facts and Figures. 2018, https://www.alz.org/alzheimers-dementia/facts-figures.
(2) Selkoe, D. J.; Hardy, J. The Amyloid Hypothesis of Alzheimer's Disease at 25 Years. *EMBO Mol. Med.* **2016**, *8*, 595−608.
(3) Cline, E. N.; Bicca, M. A.; Viola, K. L.; Klein, W. L. The Amyloid-β Oligomer Hypothesis: Beginning of the Third Decade. *J. Alzheimers Dis.* **2018**, *64*, S567−S610.
(4) Tang, W. J. Targeting Insulin-Degrading Enzyme to Treat Type 2 Diabetes Mellitus. *Trends Endocrinol. Metab.* **2016**, *27*, 24−34.
(5) Kurochkin, I. V.; Guarnera, E.; Berezovsky, I. N. Insulin-Degrading Enzyme in the Fight against Alzheimer's Disease. *Trends Pharmacol. Sci.* **2018**, *39*, 49−58.
(6) Shen, Y.; Joachimiak, A.; Rosner, M. R.; Tang, W. J. Structures of Human Insulin-Degrading Enzyme Reveal a New Substrate Recognition Mechanism. *Nature* **2006**, *443*, 870−874.
(7) Guo, Q.; Manolopoulou, M.; Bian, Y.; Schilling, A. B.; Tang, W. J. Molecular Basis for the Recognition and Cleavages of IGF-II, TGF-α, and Amylin by Human Insulin-Degrading Enzyme. *J. Mol. Biol.* **2010**, *395*, 430−443.
(8) Manolopoulou, M.; Guo, Q.; Malito, E.; Schilling, A. B.; Tang, W. J. Molecular Basis of Catalytic Chamber-Assisted Unfolding and Cleavage of Human Insulin by Human Insulin-Degrading Enzyme. *J. Biol. Chem.* **2009**, *284*, 14177−14188.
(9) Noinaj, N.; Bhasin, S. K.; Song, E. S.; Scoggin, K. E.; Juliano, M. A.; Juliano, L.; Hersh, L. B.; Rodgers, D. W. Identification of the Allosteric Regulatory Site of Insulysin. *PLoS One* **2011**, *6*, No. e20864.
(10) Kurochkin, I. V.; Guarnera, E.; Wong, J. H.; Eisenhaber, F.; Berezovsky, I. N. Toward Allosterically Increased Catalytic Activity of Insulin-Degrading Enzyme against Amyloid Peptides. *Biochemistry* **2017**, *56*, 228−239.
(11) Durham, T. B.; Toth, J. L.; Klimkowski, V. J.; Cao, J. X.; Siesky, A. M.; Alexander-Chacko, J.; Wu, G. Y.; Dixon, J. T.; McGee, J. E.; Wang, Y.; Guo, S. Y.; Cavitt, R. N.; Schindler, J.; Thibodeaux, S. J.; Calvert, N. A.; Coghlan, M. J.; Sindelar, D. K.; Christe, M.; Kiselyov, V. V.; Michael, M. D.; Sloop, K. W. Dual Exosite-Binding Inhibitors of Insulin-Degrading Enzyme Challenge Its Role as the Primary Mediator of Insulin Clearance in vivo. *J. Biol. Chem.* **2015**, *290*, 20044−20059.
(12) Zhang, Z.; Liang, W. G.; Bailey, L. J.; Tan, Y. Z.; Wei, H.; Wang, A.; Farcasanu, M.; Woods, V. A.; McCord, L. A.; Lee, D.; Shang, W.; Deprez-Poulain, R.; Deprez, B.; Liu, D. R.; Koide, A.; Koide, S.; Kossiakoff, A. A.; Li, S.; Carragher, B.; Potter, C. S.; Tang, W. J. Ensemble CryoEM Elucidates the Mechanism of Insulin Capture and Degradation by Human Insulin Degrading Enzyme. *eLife* **2018**, *7*, No. e33572.
(13) Saido, T.; Leissring, M. A. Proteolytic Degradation of Amyloid β-Protein. *Cold Spring Harbor Perspect. Med.* **2012**, *2*, No. a006379.
(14) Farris, W.; Mansourian, S.; Chang, Y.; Lindsley, L.; Eckman, E. A.; Frosch, M. P.; Eckman, C. B.; Tanzi, R. E.; Selkoe, D. J.; Guenette, S. Insulin-Degrading Enzyme Regulates the Levels of Insulin, Amyloid β-Protein, and the β-Amyloid Precursor Protein Intracellular Domain in vivo. *Proc. Natl. Acad. Sci. U.S.A.* **2003**, *100*, 4162−4167.
(15) Miller, B. C.; Eckman, E. A.; Sambamurti, K.; Dobbs, N.; Chow, K. M.; Eckman, C. B.; Hersh, L. B.; Thiele, D. L. Amyloid-β Peptide Levels in Brain Are Inversely Correlated with Insulysin Activity Levels in vivo. *Proc. Natl. Acad. Sci. U.S.A.* **2003**, *100*, 6221−6226.
(16) Stargardt, A.; Gillis, J.; Kamphuis, W.; Wiemhoefer, A.; Kooijman, L.; Raspe, M.; Benckhuijsen, W.; Drijfhout, J. W.; Hol, E. M.; Reits, E. Reduced Amyloid-β Degradation in Early Alzheimer's Disease but Not in the APPswePS1dE9 and 3xTg-AD Mouse Models. *Aging Cell* **2013**, *12*, 499−507.
(17) Wang, J.; Bi, W.; Cheng, A.; Freire, D.; Vempati, P.; Zhao, W.; Gong, B.; Janle, E. M.; Chen, T. Y.; Ferruzzi, M. G.; Schmeidler, J.; Ho, L.; Pasinetti, G. M. Targeting Multiple Pathogenic Mechanisms with Polyphenols for the Treatment of Alzheimer's Disease-Experimental Approach and Therapeutic Implications. *Front. Aging Neurosci.* **2014**, *6*, 1−9.
(18) Lakey-Beitia, J.; Berrocal, R.; Rao, K. S.; Durant, A. A. Polyphenols as Therapeutic Molecules in Alzheimer's Disease through Modulating Amyloid Pathways. *Mol. Neurobiol.* **2015**, *51*, 466−479.
(19) Pasinetti, G. M.; Wang, J.; Ho, L.; Zhao, W.; Dubner, L. Roles of Resveratrol and Other Grape-Derived Polyphenols in Alzheimer's Disease Prevention and Treatment. *Biochim. Biophys. Acta* **2015**, *1852*, 1202−1208.
(20) Orallo, F. Comparative Studies of the Antioxidant Effects of *Cis*- and *Trans*-Resveratrol. *Curr. Med. Chem.* **2006**, *13*, 87−98.
(21) Orgogozo, J. M.; Dartigues, J. F.; Lafont, S.; Letenneur, L.; Commenges, D.; Salamon, R.; Renaud, S.; Breteler, M. B. Wine Consumption and Dementia in the Elderly: A Prospective Community Study in the Bordeaux Area. *Rev. Neurol.* **1997**, *153*, 185−192.
(22) Krikorian, R.; Nash, T. A.; Shidler, M. D.; Shukitt-Hale, B.; Joseph, J. A. Concord Grape Juice Supplementation Improves Memory Function in Older Adults with Mild Cognitive Impairment. *Br. J. Nutr.* **2010**, *103*, 730−734.
(23) Krikorian, R.; Boespflug, E. L.; Fleck, D. E.; Stein, A. L.; Wightman, J. D.; Shidler, M. D.; Sadat-Hossieny, S. Concord Grape Juice Supplementation and Neurocognitive Function in Human Aging. *J. Agric. Food Chem.* **2012**, *60*, 5736−5742.
(24) Wang, J.; Ho, L.; Zhao, Z.; Seror, I.; Humala, N.; Dickstein, D. L.; Thiyagarajan, M.; Percival, S. S.; Talcott, S. T.; Pasinetti, G. M. Moderate Consumption of Cabernet Sauvignon Attenuates Aβ Neuropathology in a Mouse Model of Alzheimer's Disease. *FASEB J.* **2006**, *20*, 2313−2320.
(25) Vingtdeux, V.; Giliberto, L.; Zhao, H.; Chandakkar, P.; Wu, Q.; Simon, J. E.; Janle, E. M.; Lobo, J.; Ferruzzi, M. G.; Davies, P.; Marambaud, P. AMP-Activated Protein Kinase Signaling Activation by Resveratrol Modulates Amyloid-β Peptide Metabolism. *J. Biol. Chem.* **2010**, *285*, 9100−9113.
(26) Porquet, D.; Casadesus, G.; Bayod, S.; Vicente, A.; Canudas, A. M.; Vilaplana, J.; Pelegri, C.; Sanfeliu, C.; Camins, A.; Pallas, M.; del Valle, J. Dietary Resveratrol Prevents Alzheimer's Markers and Increases Life Span in Samp8. *AGE* **2013**, *35*, 1851−1865.
(27) Ladiwala, A. R.; Lin, J. C.; Bale, S. S.; Marcelino-Cruz, A. M.; Bhattacharya, M.; Dordick, J. S.; Tessier, P. M. Resveratrol Selectively Remodels Soluble Oligomers and Fibrils of Amyloid Aβ into Off-Pathway Conformers. *J. Biol. Chem.* **2010**, *285*, 24228−24237.
(28) Fu, Z.; Aucoin, D.; Ahmed, M.; Ziliox, M.; Van Nostrand, W. E.; Smith, S. O. Capping of Aβ42 Oligomers by Small Molecule Inhibitors. *Biochemistry* **2014**, *53*, 7893−7903.
(29) Marambaud, P.; Zhao, H.; Davies, P. Resveratrol Promotes Clearance of Alzheimer's Disease Amyloid-β Peptides. *J. Biol. Chem.* **2005**, *280*, 37377−37382.
(30) Rege, S. D.; Geetha, T.; Broderick, T. L.; Babu, J. R. Resveratrol Protects B Amyloid-Induced Oxidative Damage and Memory Associated Proteins in H19-7 Hippocampal Neuronal Cells. *Curr. Alzheimer Res.* **2015**, *12*, 147−156.
(31) Fradinger, E. A.; Maji, S. K.; Lazo, N. D.; Teplow, D. B. Studying Amyloid β-Protein Assembly. In *Amyloid Precursor Protein: A Practical Approach*; Xia, W., Xu, H., Eds.; CRC Press: Boca Raton, 2005; pp 83−110.
(32) Farris, W.; Leissring, M. A.; Hemming, M. L.; Chang, A. Y.; Selkoe, D. J. Alternative Splicing of Human Insulin-Degrading Enzyme Yields a Novel Isoform with a Decreased Ability to Degrade Insulin and Amyloid β-Protein. *Biochemistry* **2005**, *44*, 6513−6525.
(33) Gursky, O.; Aleshkov, S. Temperature-Dependent β-Sheet Formation in β-Amyloid Aβ(1-40) Peptide in Water: Uncoupling β-Structure Folding from Aggregation. *Biochim. Biophys. Acta* **2000**, *1476*, 93−102.

DOI: 10.1021/acsomega.8b01913
ACS Omega 2018, 3, 13275−13282

(34) Fontana, A.; de Laureto, P. P.; Spolaore, B.; Frare, E.; Picotti, P.; Zambonin, M. Probing Protein Structure by Limited Proteolysis. *Acta Biochim. Pol.* **2004**, *51*, 299−321.
(35) Lazo, N. D.; Grant, M. A.; Condron, M. C.; Rigby, A. C.; Teplow, D. B. On the Nucleation of Amyloid β-Protein Monomer Folding. *Protein Sci.* **2005**, *14*, 1581−1596.
(36) Rogeberg, M.; Furlund, C. B.; Moe, M. K.; Fladby, T. Identification of Peptide Products from Enzymatic Degradation of Amyloid β. *Biochimie* **2014**, *105*, 216−220.
(37) Mukherjee, A.; Song, E.; Ehmann, M. K.; Goodman, J. P.; St Pyrek, J.; Estus, S.; Hersh, L. B. Insulysin Hydrolyzes Amyloid β Peptides to Products That Are Neither Neurotoxic nor Deposit on Amyloid Plaques. *J. Neurosci.* **2000**, *20*, 8745−8749.
(38) Song, E. S.; Hersh, L. B. Insulysin: An Allosteric Enzyme as a Target for Alzheimer's Disease. *J. Mol. Neurosci.* **2005**, *25*, 201−206.
(39) Hubin, E.; Cioffi, F.; Rozenski, J.; van Nuland, N. A.; Broersen, K. Characterization of Insulin-Degrading Enzyme-Mediated Cleavage of Aβ in Distinct Aggregation States. *Biochim. Biophys. Acta* **2016**, *1860*, 1281−1290.
(40) Portelius, E.; Zetterberg, H.; Andreasson, U.; Brinkmalm, G.; Andreasen, N.; Wallin, A.; Westman-Brinkmalm, A.; Blennow, K. An Alzheimer's Disease-Specific β-Amyloid Fragment Signature in Cerebrospinal Fluid. *Neurosci. Lett.* **2006**, *409*, 215−219.
(41) Pannee, J.; Tornqvist, U.; Westerlund, A.; Ingelsson, M.; Lannfelt, L.; Brinkmalm, G.; Persson, R.; Gobom, J.; Svensson, J.; Johansson, P.; Zetterberg, H.; Blennow, K.; Portelius, E. The Amyloid-β Degradation Pattern in Plasma-a Possible Tool for Clinical Trials in Alzheimer's Disease. *Neurosci. Lett.* **2014**, *573*, 7−12.
(42) Wälti, M. A.; Ravotti, F.; Arai, H.; Glabe, C. G.; Wall, J. S.; Bockmann, A.; Guntert, P.; Meier, B. H.; Riek, R. Atomic-Resolution Structure of a Disease-Relevant Aβ(1-42) Amyloid Fibril. *Proc. Natl. Acad. Sci. U.S.A.* **2016**, *113*, E4976−E4984.
(43) Im, H.; Manolopoulou, M.; Malito, E.; Shen, Y.; Zhao, J.; Neant-Fery, M.; Sun, C. Y.; Meredith, S. C.; Sisodia, S. S.; Leissring, M. A.; Tang, W. J. Structure of Substrate-Free Human Insulin-Degrading Enzyme (IDE) and Biophysical Analysis of ATP-Induced Conformational Switch of IDE. *J. Biol. Chem.* **2007**, *282*, 25453−25463.
(44) Song, E. S.; Juliano, M. A.; Juliano, L.; Fried, M. G.; Wagner, S. L.; Hersh, L. B. ATP Effects on Insulin-Degrading Enzyme Are Mediated Primarily through Its Triphosphate Moiety. *J. Biol. Chem.* **2004**, *279*, 54216−54220.
(45) Noinaj, N.; Song, E. S.; Bhasin, S.; Alper, B. J.; Schmidt, W. K.; Hersh, L. B.; Rodgers, D. W. Anion Activation Site of Insulin-Degrading Enzyme. *J. Biol. Chem.* **2012**, *287*, 48−57.
(46) Song, E. S.; Juliano, M. A.; Juliano, L.; Hersh, L. B. Substrate Activation of Insulin-Degrading Enzyme (Insulysin). A Potential Target for Drug Development. *J. Biol. Chem.* **2003**, *278*, 49789−94.
(47) Tundo, G. R.; Di Muzio, E.; Ciaccio, C.; Sbardella, D.; Di Pierro, D.; Polticelli, F.; Coletta, M.; Marini, S. Multiple Allosteric Sites Are Involved in the Modulation of Insulin-Degrading-Enzyme Activity by Somatostatin. *FEBS J.* **2016**, *283*, 3755−3770.
(48) Maianti, J. P.; McFedries, A.; Foda, Z. H.; Kleiner, R. E.; Du, X. Q.; Leissring, M. A.; Tang, W. J.; Charron, M. J.; Seeliger, M. A.; Saghatelian, A.; Liu, D. R. Anti-Diabetic Activity of Insulin-Degrading Enzyme Inhibitors Mediated by Multiple Hormones. *Nature* **2014**, *511*, 94−98.
(49) Kukday, S. S.; Manandhar, S. P.; Ludley, M. C.; Burriss, M. E.; Alper, B. J.; Schmidt, W. K. Cell-Permeable, Small-Molecule Activators of the Insulin-Degrading Enzyme. *J. Biomol. Screen.* **2012**, *17*, 1348−61.
(50) Sharma, S. K.; Chorell, E.; Steneberg, P.; Vernersson-Lindahl, E.; Edlund, H.; Wittung-Stafshede, P. Insulin-Degrading Enzyme Prevents α-Synuclein Fibril Formation in a Nonproteolytical Manner. *Sci. Rep.* **2015**, *5*, No. 12531.
(51) Calderon, A. A.; Zapata, J. M.; Munoz, R.; Pedreno, M. A.; Barcelo, A. R. Resveratrol Production as Part of the Hypersensitive-Like Response of Grapevine Cells to an Elicitor from *Trichoderma Viride*. *New Phytol.* **1993**, *124*, 455−463.

DOI: 10.1021/acsomega.8b01913
ACS Omega 2018, 3, 13275−13282